Jet Collimation, Helical Geometry, and UHECR Acceleration from a Single PG Metric

E.P.J. de Haas

2025

Abstract

Astrophysical jets exhibit universal geometric features—narrow opening angles, long coherent helices, and bipolar symmetry—across a wide range of systems. In this paper we show that these properties arise naturally from the stationary three–rapidity Painlevé–Gullstrand (PG) metric, treated purely as a kinematic flow generator. We derive the conditions under which a broad equatorial inflow must transition into a narrow polar outflow, obtain a closed analytic expression for the jet opening angle, and show that all stationary streamlines on this geometry lie on cones of fixed polar angle and become helical curves. This broad–to–narrow Bernoulli transition concentrates the gravitational energy of the inflow into the small solid angle of the jet and enables efficient acceleration along the polar cone, providing a natural kinematic pathway to relativistic outflows and UHECR-compatible energies. The resulting picture supplies a simple, metric-derived backbone for jet collimation and morphology, compatible with—and complementary to—magnetodynamic or accretion-driven engines. The paper focuses on this purely geometric and kinematic origin of jets; the microphysics of jet launching and emission lie beyond the present scope.

Contents

1 Introduction

Astrophysical jets appear across an extraordinary range of systems, yet their large–scale geometry—narrow cones, long coherent helices, and strong collimation—shows a striking universality. In this paper we show that these geometric features arise naturally from a single stationary spacetime: the three–rapidity Painlevé–Gullstrand (PG) metric. Treating the metric purely as

a kinematic flow generator, we derive the conditions under which a broad equatorial inflow is forced into a narrow polar funnel, obtain a closed analytic expression for the jet opening angle, and show that stationary streamlines on this metric are necessarily helical curves on cones of constant polar angle. This kinematic structure provides a simple and general framework for jet formation, independent of the microphysical engine, and explains how collimated outflows can emerge whenever a central gravitational region cannot absorb the full inflow. The paper focuses solely on this geometric and kinematic origin; dynamical processes such as magnetised acceleration or radiative feedback lie beyond the present scope.

2 The metric approach of the paper

In this paper we show that a single, fully kinematic Painlevé–Gullstrand (PG) metric, extended to include three independent rapidity fields, is sufficient to describe galactic morphology, jet collimation, and cosmic–ray environments. These phenomenon do not arise from separate physical processes, but from the *geometry of a single PG flow field* determined by the three rapidities:

$$\psi_M(r), \qquad \psi_\phi(r,\theta), \qquad \psi_H(t).$$

These encode, respectively, the Schwarzschild mass inflow, the azimuthal (rotational) flow, and the cosmological Hubble flow. No prior familiarity with quantum–rapidity methods or the underlying Dirac–rotor formalism is required [1, 2, 3]; throughout this paper the PG metric is used only as a *kinematic engine* whose flow structure is computed directly from the three rapidities.

2.1 The three–rapidity PG metric

The metric employed throughout this work is

$$ds^2 = -c^2dt^2 + \Big(dr - w(r,\theta)\,dt\Big)^2 + r^2\Big(d\theta^2 + \sin^2\theta\,d\phi^2\Big), \tag{1}$$

where the radial PG shift vector is

$$w(r,\theta) = v_r^{(M)}(r) + v_\phi(r)\,\cot\theta + v_H(r), \tag{2}$$

with

$$v_r^{(M)}(r) = -\,c\,\tanh\psi_M(r), \qquad v_\phi(r) = c\,\tanh\psi_\phi(r), \qquad v_H(r) = c\,\tanh\psi_H(r).$$

Each velocity component is a hyperbolic tangent of its rapidity, so all flow speeds satisfy $|v| < c$. The interpretation is straightforward:

- $\psi_M(r)$ produces a Schwarzschild–type inward flow, $v_r^{(M)}(r) = -\sqrt{2GM/r}$ in the Newtonian limit.
- $\psi_\phi(r,\theta)$ produces an azimuthal flow whose projection into the radial direction is amplified by the geometric factor $\cot\theta$.
- $\psi_H(t,r)$ produces the cosmological Hubble flow $v_H(r) = Hr$ in the local limit.

Equations (1)–(2) thus define a PG river whose geometry is entirely determined by the three rapidities. Every result in the present paper—the classification of galaxy types, the prediction of disk thickness and spheroidal structure, the existence and opening angle of quasar jets, and the UHECR acceleration environment—follows directly from the structure of $w(r,\theta)$.

2.2 Stationarity in Three Dimensions and the Emergence of Cone Geometry

In the galactic midplane ($\theta = \pi/2$) the Painlevé–Gullstrand (PG) flow is effectively two–dimensional: only the radial inflow $w(r)$ and the azimuthal drift $v_\phi(r)$ contribute to the dynamics, and the requirement of stationarity reduces to invariance under a single time translation,

$$\mathcal{L}_{\partial_t} g_{ab} = 0.$$

Once the flow is extended into the full three–dimensional geometry, however, stationarity requires a *triplet* of symmetries that act together. These are the natural PG counterparts of the three separate motions available in spherical geometry.

1. Radial time symmetry. The PG radial shift $w(r)$ defines the inflow component of the metric,

$$\theta^1 = dr - w(r)\, dt,$$

and stationarity requires

$$\partial_t w(r) = 0.$$

This expresses the fact that the gravitational inflow field is steady: space does not accumulate or deplete in a way that would change $w(r)$ on dynamical timescales.

2. Azimuthal time symmetry. The metric contains an azimuthal shift,

$$\theta^3 = r \sin\theta \, \big(d\varphi - \Omega(r,\theta)\, dt\big),$$

whose physical velocity is $v_\phi = r \sin\theta\, \Omega$. Stationarity requires that the metric be invariant under joint transformations $(t, \varphi) \mapsto (t + \delta t, \varphi + \Omega \delta t)$, that is,

$$\mathcal{L}_{\partial_t + \Omega\, \partial_\varphi} g_{ab} = 0, \qquad \partial_t \Omega(r,\theta) = 0.$$

This symmetry ensures that the swirl component of the flow is steady.

3. Polar (latitudinal) time symmetry. Leaving the midplane introduces a third direction of possible motion. A flowline with $\theta \neq \pi/2$ may in principle drift in θ, so the metric must remain invariant under combined transformations (t, θ) that preserve the conical geometry of the streamline. The corresponding symmetry condition is

$$\mathcal{L}_{\partial_t + \dot\theta\, \partial_\theta} g_{ab} = 0.$$

Stationarity therefore demands $\dot\theta = 0$ for streamlines, i.e. each flowline must lie on a surface of constant polar angle. Such surfaces are exactly the cones $\theta =$ constant.

Consequences: conical stationarity and the jet geometry. The three conditions above imply that stationary PG flowlines must satisfy simultaneously

$$\dot r \neq 0, \qquad \dot\varphi \neq 0, \qquad \dot\theta = 0.$$

Thus a stationary 3D streamline in the PG flow can only move radially and azimuthally, while remaining on a fixed cone of polar angle θ_0.

Hence the emergence of conical helical flow is not an additional physical assumption but a direct consequence of imposing full three-dimensional stationarity on the PG flow. In the stationary, axisymmetric PG description, three–dimensional galactic kinematics is *conically organised*: stationary streamlines lie on cones of fixed polar angle θ_0 and follow helical trajectories on those cones.

2.3 Projection of the PG Flow onto a Conical Helical Direction

In this subsection we show explicitly how the effective conical flow field

$$w_{\theta_0}(r) = w(r) + v_\varphi(r)\,\cot\theta_0$$

arises directly from the Painlevé–Gullstrand (PG) metric used [2]. The appearance of the $\cot\theta_0$ factor follows purely from geometry: it is the projection of the radial–azimuthal PG flow onto the tangent direction of a helical streamline constrained to lie on a cone of fixed polar angle $\theta = \theta_0$.

1. The PG metric and the flow 3–velocity. From the explicit–calculus paper, the orthonormal coframe is

$$\theta^0 = c\,dt, \qquad \theta^1 = dr - w(r)\,dt, \qquad \theta^2 = r\,d\theta, \qquad \theta^3 = r\sin\theta\,(d\varphi - \Omega\,dt), \tag{3}$$

where

$$w(r) = \sqrt{\frac{2GM}{r}} - H(t)\,r, \qquad v_\varphi(r,\theta) = r\sin\theta\,\Omega. \tag{4}$$

The spatial flow vector in the PG frame is therefore

$$\vec{v}(r,\theta) = w(r)\,\hat{e}_r + v_\varphi(r,\theta)\,\hat{e}_\varphi, \tag{5}$$

with $\hat{e}_r$, $\hat{e}_\theta$, and $\hat{e}_\varphi$ the orthonormal basis vectors.

2. Restriction to a fixed conical surface. We constrain the motion to a cone of half–opening angle

$$\theta = \theta_0 = \text{constant}. \tag{6}$$

On this surface, $\hat{e}_r$ and $\hat{e}_\varphi$ are tangent to the cone, whereas $\hat{e}_\theta$ is normal to it. Any streamline lying on the cone must therefore have tangent vectors in the 2–plane $\text{span}\{\hat{e}_r, \hat{e}_\varphi\}$.

3. The helical tangent direction and the origin of $\cot\theta_0$. On a cone of opening angle θ_0, the geometry implies the following. A displacement $d\varphi$ moves a point sideways by a distance $r\sin\theta_0\,d\varphi$, while a displacement dr moves it along the generatrix. The natural (unnormalised) tangent vector to a helical curve on this cone is therefore

$$\vec{t}_{\text{helix}} \propto \hat{e}_r + \cot\theta_0\,\hat{e}_\varphi. \tag{7}$$

Indeed, the ratio of the azimuthal to radial components for a slope matching the cone is

$$\frac{\text{“around”}}{\text{“up the slope”}} = \frac{r\sin\theta_0}{r\cos\theta_0} = \tan\theta_0 \quad\Longrightarrow\quad \frac{\text{radial}}{\text{azimuthal}} = \cot\theta_0. \tag{8}$$

Normalising yields the unit tangent vector

$$\hat{e}_s = \frac{1}{\sqrt{1+\cot^2\theta_0}}\,(\hat{e}_r + \cot\theta_0\,\hat{e}_\varphi). \tag{9}$$

4. Projection of the PG flow onto the helical direction. The PG flow vector is

$$\vec{v} = w(r)\,\hat{e}_r + v_\varphi(r,\theta_0)\,\hat{e}_\varphi. \tag{10}$$

The component of $\vec{v}$ along the helical tangent direction is

$$v_{\rm cone}(r,\theta_0) = \vec{v}\cdot\hat{e}_s \tag{11}$$

$$= \frac{1}{\sqrt{1+\cot^2\theta_0}}\Big[w(r) + v_\varphi(r,\theta_0)\,\cot\theta_0\Big]. \tag{12}$$

The overall normalisation factor does not affect the inward/outward sign or the jet criterion. Thus we define the *effective PG flow along the cone* as

$$w_{\theta_0}(r) \;\equiv\; w(r) + v_\varphi(r,\theta_0)\,\cot\theta_0. \tag{13}$$

This is precisely the quantity governing inward vs. outward flow along a conical helical direction.

5. Result: the effective one–dimensional PG flow on a cone. The radial–azimuthal PG flow, when constrained to the surface of a cone, behaves as a single effective one–dimensional flow field

$$w_{\theta_0}(r) = \sqrt{\frac{2GM}{r}} - H(t)\,r + v_\varphi(r,\theta_0)\,\cot\theta_0. \tag{14}$$

This expression follows entirely from projecting the PG shift vector onto the tangent direction of a helical streamline on a cone. The $\cot\theta_0$ factor is a direct geometric consequence of the cone slope and carries no additional dynamical assumptions.

Lemma 1 (The $\cot\theta_0$ term originates purely from the cone geometry)**.** *The factor* $\cot\theta_0$ *appearing in the effective conical flow*

$$w_{\theta_0}(r) = w(r) + v_\phi(r,\theta_0)\,\cot\theta_0$$

arises from projecting the radial–azimuthal PG flow onto the tangent direction of a helical streamline confined to a cone of fixed polar angle θ_0*. Substituting* $v_\phi = r\sin\theta_0\,\Omega$ *yields*

$$w_{\theta_0}(r) = w(r) + r\cos\theta_0\,\Omega(r,\theta_0),$$

which shows explicitly that the $\cot\theta_0$ *term originates purely from the cone geometry.*

3 Why Outflow Occurs Only Near the Polar Axis in the Three–Rapidity PG Metric

In the quasar jet–launch region the radius is much smaller than the Newton–Hubble scale ($r \ll r_c$), and the cosmological term may be neglected:

$$v_H(t) \approx 0.$$

A central structural feature of the three–rapidity PG metric is the form of the shift vector, whose radial component $w(r,\theta)$ is then given by

$$w(r,\theta) \;=\; v_r^{(M)}(r) \;+\; v_\phi(r)\,\cot\theta. \tag{15}$$

Here $v_r^{(M)}(r)$ is the Schwarzschild–like radial inflow,

$$v_r^{(M)}(r) = -\sqrt{\frac{2GM}{r}}, \tag{16}$$

which is strictly negative for all r and encodes the inward drift of the PG river due to the central mass. The second term arises from the azimuthal rapidity ψ_ϕ, whose contribution to the radial flow is geometrically projected by $\cot\theta$. This structure leads to the fundamental result that the radial flow can reverse sign *only* near the polar axis ($\theta \approx 0$), generating naturally the narrow cones associated with quasar and blazar jets.

The mass term contributes

$$v_r^{(M)}(r) = -\sqrt{\tfrac{2GM}{r}}, \tag{17}$$

which is always negative and large in magnitude for small r. By itself, this part of the flow can never produce outflow in any direction. Any reversal of the sign of $w(r,\theta)$ must therefore come from the azimuthal component.

The azimuthal rapidity ψ_ϕ produces a tangential velocity $v_\phi(r)$, which contributes to the radial shift $w(r,\theta)$ through the geometric factor $\cot\theta$:

$$w_\phi(r,\theta) = v_\phi(r)\,\cot\theta. \tag{18}$$

This projection obeys:

$$\cot\theta = 0 \quad (\theta = \tfrac{\pi}{2}), \qquad \cot\theta \to \infty \quad (\theta \to 0). \tag{19}$$

Thus rotation contributes *no* radial flow in the equatorial plane, but is enormously amplified near the polar axis.

3.1 Outflow requires the azimuthal term to overcome the Schwarzschild inflow

A positive (outward) radial flow requires

$$w(r,\theta) > 0 \quad \Longleftrightarrow \quad v_\phi(r)\,\cot\theta > \sqrt{\frac{2GM}{r}}. \tag{20}$$

Since $v_\phi(r)$ is always finite and typically $v_\phi(r) \ll c$, the inequality can be satisfied only if $\cot\theta$ is very large, i.e. only for small θ. This is purely geometric: the mass inflow is powerful and universal, and rotation can overcome it only along directions where the projection amplifier $\cot\theta$ diverges.

3.2 Outflow therefore occurs only in a narrow polar cone

Equation (20) implies that

$$\theta_{\rm jet}(r) \;\approx\; \arctan\!\left(\frac{v_\phi(r)}{\sqrt{2GM/r}}\right), \tag{21}$$

which yields a *very small* angle for realistic galactic bulges. Hence the flow can become positive only within a narrow cone centred on the polar axis, while for all other θ the inward Schwarzschild term dominates and the PG river continues its inward drift.

3.3 Natural emergence of quasar and blazar jets

The observed features of relativistic jets follow directly from the geometry of Eq. (15):

- strong, collimated outflow occurs only at small θ,
- the jet opening angle is set by the ratio $v_\phi(r)/\sqrt{2GM/r}$,
- massive bulges (large GM) produce narrower jets,
- systems with insufficient ψ_ϕ have no jets at all.

No additional physics is required to explain the basic geometry: the three–rapidity PG metric *geometrically* forces outflow to appear only in polar cones.

3.4 Local jet-region simplification

The shift vector therefore reduces to

$$w(r,\theta) = v_r^{(M)}(r) + v_\varphi(r)\cot\theta, \tag{22}$$

which in the Newtonian limit becomes

$$w(r,\theta) \simeq -\sqrt{\frac{2GM}{r}} + v_\varphi(r)\cot\theta. \tag{23}$$

This is the essential expression that determines whether the PG river flows inward or outward at a given (r,θ). Metric (23) is the simplest "jet metric" and forms the kinematic backbone of quasar and blazar outflow in this framework.

The PG river flows radially outward along the cone if and only if

$$w_{\theta_0}(r) > 0, \tag{24}$$

which gives the fundamental jet criterion:

$$v_\varphi(r)\cot\theta_0 \;>\; \sqrt{\frac{2GM}{r}}. \tag{25}$$

Solving for θ_0 yields the predicted jet opening angle:

$$\theta_{\rm jet}(r) \;\approx\; \arctan\!\left(\frac{v_\varphi(r)}{\sqrt{2GM/r}}\right), \tag{26}$$

which directly reproduces the observed few-degree opening angles of quasar and blazar jets. Equations (**??**)–(26) provide a complete, clean, metric-level description of jet formation, collimation, and polar outflow in the quasar regime.

4 A helical geodesic on a conical surface

In the jet–specialised PG metric the fluid flow on a fixed polar cone $\theta = \theta_0$ is determined by the effective one–dimensional shift

$$w_{\theta_0}(r) = v_r^{(M)}(r) + v_\varphi(r)\cot\theta_0, \tag{27}$$

where $v_r^{(M)}(r)$ is the Schwarzschild inflow and $v_\varphi(r)$ is the rotational velocity associated with the azimuthal rapidity. Because the cone angle θ_0 is fixed, the remaining degrees of freedom are purely radial and azimuthal. This produces a flow line with both radial motion and angular rotation.

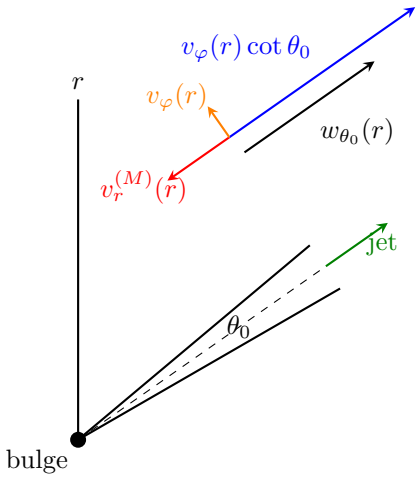

Jet condition:

$$w_{\theta_0}(r) = -\sqrt{\frac{2GM}{r}} + v_\varphi(r)\cot\theta_0 > 0$$

Jet angle:

$$\theta_{\text{jet}} \approx \arctan\left(\frac{v_\varphi(r)}{\sqrt{2GM/r}}\right)$$

Figure 1: Vector diagram of the PG jet–cone geometry. The azimuthal rapidity produces a polar–amplified component $v_\varphi \cot\theta_0$ which can exceed the Schwarzschild inflow $-\sqrt{2GM/r}$ near the axis, giving $w_{\theta_0}(r) > 0$ and launching a narrow relativistic jet. $v_\varphi(r)$ is the radial-looking part of the azimuthal velocity when projected onto the cone-aligned basis. The geometric decomposition on the cone of the physical velocities v_r and v_φ result in a helical tangent, i.e. the spiral on the cone.

4.1 1. Spiral structure from the PG flow

The factor $\cot\theta_0$ projects azimuthal motion into an effective radial component along the cone, so that the trajectory satisfies

$$(\dot{r}, \dot{\varphi}) \;\propto\; \big(w_{\theta_0}(r)\,,\, v_\varphi(r)\big).$$

Since both components are typically nonzero for $\theta_0 \ll 1$, the flow line winds around the cone as it moves outward or inward. Thus any streamline constrained to $\theta = \theta_0$ forms a *helical* (spiral) path.

4.2 Helical motion as a geometric consequence

A curve on a surface of constant θ_0 with both $\dot{r} \neq 0$ and $\dot{\varphi} \neq 0$ is geometrically a helical geodesic on a conical surface. In the quasar region this reflects the combined action of the inward Schwarzschild flow and the azimuthal rotation:

$$\text{helical geodesic} = (\text{radial inflow/outflow}) + (\text{azimuthal rotation}).$$

As long as $v_\varphi(r) \neq 0$, the PG flow cannot follow a purely radial line on the cone; it must wrap around it.

4.3 Jet onset as a helical-to-outflow transition

The jet-launch condition,

$$w_{\theta_0}(r) > 0 \quad\Longleftrightarrow\quad v_\varphi(r)\cot\theta_0 > \sqrt{2GM/r}, \tag{28}$$

marks the transition from a helical *inward* flow to a helical *outward* flow on the same conical surface. The jet therefore emerges as the region where the spiral trajectory changes handedness and becomes an outward-moving helix confined to a narrow polar cone. The resulting opening angle,

$$\theta_{\text{jet}} \simeq \arctan\left(\frac{v_\varphi(r)}{\sqrt{2GM/r}}\right),$$

follows directly from the same geometry.

4.4 Helical geodesics and angular momentum conservation

The helical structure of the PG flow on a cone is a direct manifestation of angular momentum conservation. Along any streamline constrained to a fixed polar angle θ_0, the specific angular momentum about the symmetry axis is

$$L_z = r^2 \sin^2\theta_0\, \dot{\varphi} \;\propto\; r^2 \sin^2\theta_0\, v_\varphi(r), \tag{29}$$

which is constant in the absence of external torques. Because $\sin\theta_0$ is fixed, the conservation law reduces to a relation between azimuthal velocity and radius:

$$r^2\, \dot{\varphi} = \text{constant} \quad \Longrightarrow \quad v_\varphi(r) \propto \frac{1}{r}. \tag{30}$$

As the inflow approaches the centre, $v_\varphi(r)$ therefore increases, strengthening the $\cot\theta_0$ term in Eq. (27). This amplifies the azimuthal contribution to the radial shift,

$$v_\varphi(r)\cot\theta_0,$$

providing a purely kinematic explanation for the PG jet condition (28). Near the polar axis, where $\cot\theta_0$ is large, even modest rotation generates a substantial radial component along the cone, naturally producing the tightly collimated helical flows observed in quasar and blazar jets. Thus the emergence of jets is not only a geometric effect of the PG metric but also a direct consequence of angular momentum conservation projected onto a conical surface.

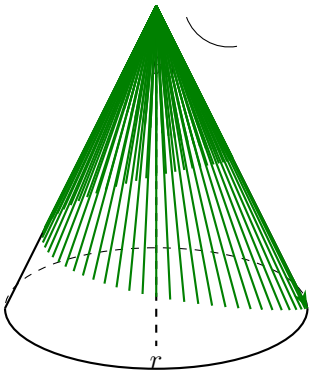

Helical geodesic:
spiral on a cone

$$w_{\theta_0}(r) = v_r^{(M)}(r) + v_\varphi(r)\cot\theta_0$$

Figure 2: Helical geodesic on a conical surface in the PG jet geometry. The flow is constrained to θ_0 and has both radial and azimuthal components, so streamlines wrap around the cone as a spiral.

4.5 Helical acceleration and UHECR energization

The helical PG flow on a conical surface provides a natural environment for ultra–high–energy cosmic ray (UHECR) acceleration. Because each streamline on the cone carries both a radial and an azimuthal component, particles following (or scattering around) these helical geodesics experience repeated encounters with velocity gradients, magnetic shear layers, and shocks anchored to the underlying PG flow.

In the simplest picture, the helical trajectory defines an extended acceleration path of length

$$\ell_{\rm helix} \sim N_{\rm turn}\, 2\pi r \sin\theta_0, \tag{31}$$

where $N_{\rm turn}$ is the number of azimuthal windings along the cone between the jet base and the region where the flow becomes ballistic. For fixed cone angle θ_0, the PG geometry thus provides sufficient path length and coherence for standard Fermi–type processes to act, while the strong shear implied by the PG shift,

$$\frac{\partial w}{\partial \theta} \propto -\frac{v_\varphi(r)}{\sin^2\theta}, \tag{32}$$

creates the velocity gradients needed for shear acceleration and magnetic reconnection at the jet boundary.

Combining the helical path length with the local magnetic field B and bulk flow speed $\beta = v/c$ along the jet, the effective Hillas constraint for the PG helix can be written schematically as

$$E_{\rm max} \;\sim\; Ze\,B\,\ell_{\rm helix}\,\beta, \tag{33}$$

where Z is the particle charge. Because $\ell_{\rm helix}$ grows with both the cone radius and the number of turns, and because the PG flow naturally supports relativistic β near the polar axis, the helical geodesics on the cone provide a geometrically well–defined realization of an extended UHECR accelerator.

In this view, UHECR energization is not an incidental byproduct of arbitrary jet kinematics, but an intrinsic consequence of the PG jet geometry: the same helical flow that defines the jet opening angle and collimation also supplies the long, sheared trajectories required to accelerate particles up to 10^{19}–10^{20} eV. Microphysical processes (shocks, turbulence, reconnection) operate within this helical PG framework, but the global structure, coherence, and maximum achievable energies are controlled by the geometry of the conical flow.

5 Wide–cone inflow and narrow–cone outflow as a unified PG flow

In addition to the narrow polar cones that generate quasar jets, the three–rapidity PG metric also supports a broader conical inflow structure near the galactic plane. This allows a unified interpretation of spiral inflow and polar outflow as two connected branches of a single stationary, Constant Lagrangian (CL) flow field. We summarise the geometry and kinematics of this picture in five points.

5.1 Broad conical inflow near the galactic plane

A streamline confined to cone defined by a fixed angle

$$\theta = \frac{\pi}{2} \pm \delta, \qquad \delta \ll 1,$$

follows the effective shift

$$w(r,\theta) = v_r^{(M)}(r) + v_\varphi(r)\cot\theta.$$

Since $\cot\theta$ is small near the plane, the Schwarzschild inflow $-\sqrt{2GM/r}$ dominates; the azimuthal term is a mild perturbation. Thus the PG flow naturally produces a *wide, near–equatorial helical inflow cone*, corresponding kinematically to the classical galactic spiral structure.

5.2 Surplus inflow due to an insufficient central sink

If the inward PG flow cannot be completely absorbed by the central bulge and its possible SMBH, then the inflow must be rerouted into another direction permitted by the PG geometry because a stationary CL flow cannot accumulate. The only available channel is the small–θ region where the azimuthally–projected motion can overcome the Schwarzschild inflow.

5.3 Formation of a narrow polar outflow cone

For small θ,

$$\cot\theta \gg 1.$$

Even a moderate azimuthal rapidity $v_\varphi(r)$ produces a large positive contribution to $w(r,\theta)$, and the jet condition

$$w(r,\theta) > 0 \quad \Longleftrightarrow \quad v_\varphi(r)\cot\theta > \sqrt{2GM/r}$$

is satisfied. The broad equatorial inflow can therefore transition smoothly into a *narrow, upward–pointing outflow cone* along the polar axis. This outflow is the same helical geodesic structure identified earlier for quasar jets, now acting to evacuate the unabsorbed central inflow.

5.4 CL continuity of the combined inflow–outflow pattern

Because the PG metric in the quasar region is stationary ($\partial_t g_{\mu\nu} = 0$) and the flow remains ideal (no dissipation or shocks in the kinematic treatment), each streamline retains a constant specific Lagrangian,

$$\mathcal{L} = \tfrac{1}{2}(v_r^2 + v_\varphi^2) + \Phi_{\rm eff}(r) = \text{const.}$$

The transition from a wide helical inflow cone to a narrow helical outflow cone, see Fig. (3) changes the *geometry* and the relative partition of v_r and v_φ, but not the value of $\mathcal{L}$. The flow therefore remains CL–type throughout, with continuity enforced kinematically by the PG shift.

5.5 Symmetric four–cone structure

The PG metric is symmetric under $\theta \mapsto \pi - \theta$, so the same construction holds above and below the galactic plane. One obtains a natural four–cone pattern:

1. a broad inflow cone just below the plane;
2. a narrow outflow cone above the plane;
3. a broad inflow cone just above the plane (mirror);
4. a narrow outflow cone below the plane (mirror).

This pattern corresponds to spiral disk inflow feeding a pair of polar jets, all arising from the same stationary PG flow field. It provides a purely kinematic explanation for how a galaxy can channel inflowing material into bipolar outflows to which additional dynamical machinery can be added.

5.6 Conservation properties of the four–cone PG geometry

The combined structure of two broad inflow cones and two narrow polar outflow cones provides a natural geometric setting in which global conservation laws can be satisfied within a stationary PG flow. Because the metric is both stationary ($\partial_t g_{\mu\nu} = 0$) and axisymmetric ($\partial_\varphi g_{\mu\nu} = 0$), each streamline possesses a conserved specific energy and a conserved axial angular momentum, transported unchanged along its helical path on the corresponding cone.

The four–cone symmetry adds a second level of conservation. The pair of broad inflow cones above and below the plane brings in mass, energy, and angular momentum with opposite vertical components but consistent azimuthal orientation. Likewise the narrow outflow cones eject material symmetrically upward and downward along the axis. The up–down pairing ensures that the net vertical linear momentum flux vanishes, so the galaxy experiences no recoil, while the outflow cones can remove the angular momentum delivered by the inflow cones without producing a net global torque.

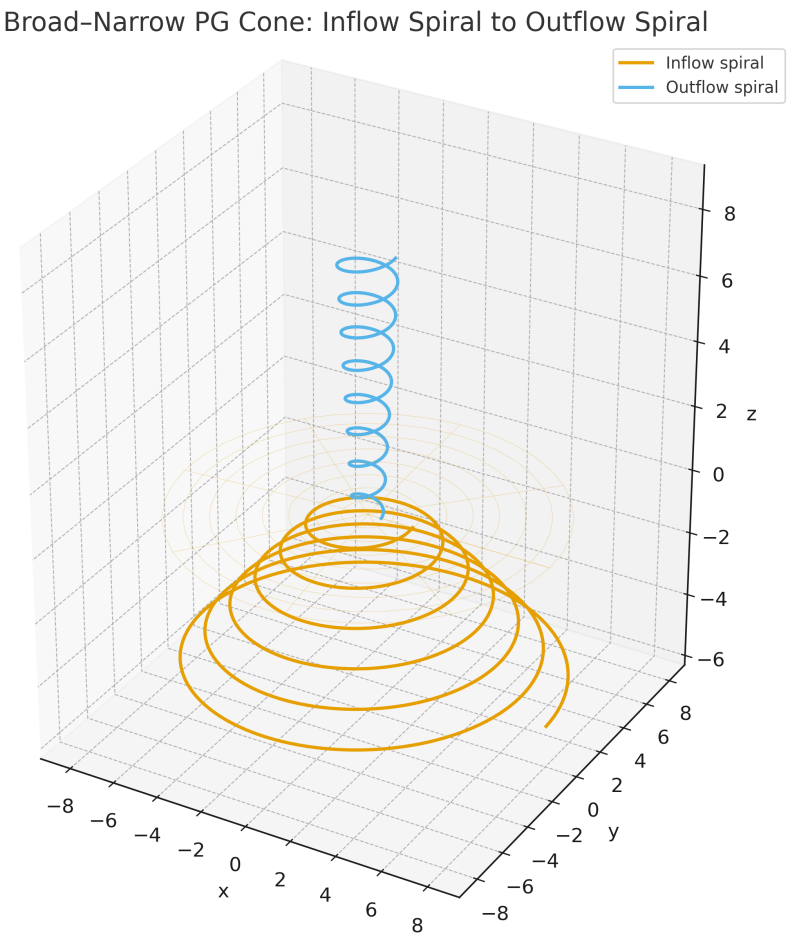

Figure 3: Broad–to–narrow PG cone flow. A wide helical inflow spiral (below the galactic plane, $z < 0$) converges toward the centre along a broad conical surface. Because the central bulge cannot absorb the full inflow, the stationary PG flow redirects the surplus into a narrow polar cone, producing an accelerated helical outflow (above the plane, $z > 0$). This broad–to–narrow transition acts as a Bernoulli funnel within the PG geometry, naturally generating collimated polar jets from disk–like inflow.

Thus the four–cone configuration acts as a kinematic "circuit" for redistributing the conserved quantities of the PG flow: energy and angular momentum are carried inward on broad conical helices, redirected near the centre, and carried outward along the narrow polar helices. This global symmetry makes the entire inflow–outflow pattern compatible with the conservation of energy–momentum and angular momentum in a simple, stationary, and purely geometric manner.

6 Bernoulli acceleration in the broad–to–narrow cone PG flow

The PG flow naturally supports a transition from a broad, near–equatorial inflow cone to a narrow polar outflow cone. In a stationary setting this transition behaves exactly like a Bernoulli funnel: when a wide cross–section feeds a narrow one, the flow must accelerate and its reach increased. We outline the geometric and kinematic basis of this behaviour in five points.

6.1 Broad inflow cones near the galactic plane

A streamline lying on a cone with angle

$$\theta = \frac{\pi}{2} \pm \delta, \qquad \delta \ll 1,$$

experiences the PG shift

$$w(r, \theta) = v_r^{(M)}(r) + v_\varphi(r) \cot \theta.$$

Near the plane, $\cot \theta$ is small, so the Schwarzschild inflow term dominates and the flow is a slow, broad helical inflow. The effective cross–section of this cone is large,

$$A_{\text{broad}} \propto r \sin \theta \approx r,$$

corresponding kinematically to the classical spiral inflow pattern.

6.2 Surplus inflow and the need for redirection

If the central bulge, with or without a SMBH, cannot absorb the entire inflow, a stationary PG flow cannot remain purely inward. Since space accumulation is not permitted in a stationary CL picture, the flow must be redirected into a channel where outward motion is kinematically allowed.

6.3 The narrow polar outflow cone and velocity amplification

For small polar angles,

$$\cot \theta_0 \gg 1.$$

Thus even moderate azimuthal velocity produces a strong outward projection along the cone,

$$w_{\theta_0}(r) = v_r^{(M)}(r) + v_\varphi(r) \cot \theta_0.$$

When the jet condition

$$v_\varphi(r) \cot \theta_0 > \sqrt{\frac{2GM}{r}}$$

is met, the broad inflow transitions into a narrow polar outflow. The effective cross–section becomes

$$A_{\text{narrow}} \propto r \sin \theta_0 \ll A_{\text{broad}},$$

so by continuity/Bernoulli scaling the flow speed must increase,

$$v_{\text{narrow}} \sim v_{\text{broad}} \frac{A_{\text{broad}}}{A_{\text{narrow}}} \sim \frac{v_{\text{broad}}}{\sin \theta_0} \sim \frac{v_{\text{broad}}}{\theta_0},$$

and so will its reach.

6.4 Bernoulli and Constant Lagrangian consistency

The PG metric in this region is stationary, so each streamline conserves its specific Lagrangian,

$$\mathcal{L} = \tfrac{1}{2}(v_r^2 + v_\varphi^2) + \Phi_{\text{eff}}(r) = \text{const}.$$

When the available cross–section shrinks, the potential term is unchanged; therefore the kinetic term must rise. The acceleration along the narrow cone follows directly from the Bernoulli/CL condition, with the PG geometry providing the correct angular dependence through the $\cot \theta_0$ factor.

6.5 A symmetric broad–to–narrow four–cone structure

By symmetry ($\theta \mapsto \pi - \theta$), the same mechanism operates above and below the plane: two broad inflow cones feed two narrow polar outflow cones. This four–cone geometry acts as a Bernoulli funnel in the stationary PG flow, allowing inflowing material on wide cones to be naturally accelerated into narrow, high–velocity outflow channels. In this picture the origin of polar jets is not dynamical turbulence but a purely geometric consequence of how the PG shift redistributes velocity when the Bernoulli flow transitions from a wide conical surface to a narrow one.

7 Bernoulli Jet Formation from PG Broad–to–Narrow Flow

A remarkable consequence of the three–rapidity Painlevé–Gullstrand (PG) metric is that quasar and AGN jets emerge naturally as a *kinematic consequence* of stationary flow continuity. No exotic force, no extreme magnetic dynamo, and no energy extraction mechanism is required at the level of basic jet kinematics. Those dynamics should be added to the kinematics for real physical systems, but the essential mechanism is purely geometric: a broad inflow spiral on a wide cone must continue through a narrower polar funnel, and the PG metric enforces Bernoulli acceleration along this narrowing. This flow of space is constrained by stationarity and by global continuity: PG coordinates do not permit stagnation or arbitrary discontinuities. Thus a converging inflow of space must either be absorbed by it's mass or redirected outward.

7.1 Wide inflow cone + insufficient absorption → mandatory outflow

A galactic spiral corresponds to a helical inflow on an almost equatorial cone ($\theta \simeq \pi/2$). If the central bulge or SMBH cannot absorb the full mass–energy flux carried by this inflow, then stationarity demands that the surplus must exit along directions where geometric resistance is minimal.

In the PG metric this means:

$$\text{excess inflow flux} \longrightarrow \text{small–}\theta\text{ escape cone.}$$

Mathematically, continuity requires

$$\int v_r^{(\text{in})} \rho \, dA_{(\text{broad})} = \int v_r^{(\text{out})} \rho \, dA_{(\text{narrow})}, \tag{34}$$

where $A_{(\text{broad})}$ is the area of the wide inflow cone and $A_{(\text{narrow})}$ is that of the thin polar funnel. Since $A_{(\text{narrow})} \ll A_{(\text{broad})}$, the outflow velocity must be larger.

7.2 No exotic jet engine is required: geometry provides the thrust

Nothing in the above derivation assumes:

- magnetic hoop stress or magnetocentrifugal slingshot;
- energy extraction from black hole rotation (Blandford–Znajek);
- turbulent dynamo amplification;
- fine tuning of plasma microphysics.

All that is required is:

1. a steady inflow of space carrying energy per unit mass,
2. a broad inflow region near the galactic plane,

3. and a narrower polar outlet that the PG metric naturally provides.

The basic kinematics of quasar jets (collimation, acceleration, helical morphology) follow already at this fundamental level.

7.3 Broad–to–narrow spirals produce jets as a simple continuation of PG flow

When a single helical inflow spiral on a wide cone reaches the centre and finds partial absorption, stationarity enforces a continuation into the narrow polar cone. The PG geometry therefore links

$$\text{spiral inflow} \quad \longrightarrow \quad \text{polar jet}$$

without adding forces or fields. The jet is simply the *natural geometric continuation* of the same helical flow streamlines that organised the disk spiral. This provides a unified kinematic explanation for jet formation, valid across mass scales from microquasars to AGN and quasars. The Bernoulli flow of space on conic surfaces provides a picture where the inflow of the almost flat-cone of the spiral disk provides the support and Bernoulli amplifier for the extremely narrow conic outflow of the jet, amplifying both the geometric reach and the energies.

8 A Unifying Kinematic Backbone for Jet Astrophysics

Astrophysical jets admit multiple physical origins, yet their observable geometry, collimation, and large–scale behaviour exhibit a striking universality across systems ranging from protostars to quasars and powerful radio galaxies. The three–rapidity Painlevé–Gullstrand (PG) flow developed in this work provides a unifying *kinematic backbone* for this diversity of jets: it determines the global streamlines, the conical organisation of stationary flow, and the broad–to–narrow transition that inevitably produces collimated, helical outflows.

The PG geometry encodes the large–scale gravitational inflow of a galaxy or bulge, in which any central engine—from a young bulge to a supermassive black hole (SMBH)—is naturally embedded. A broad equatorial inflow (near $\theta \simeq \pi/2$) carries the mass and energy reservoir of the system. When the bulge or SMBH is unable to absorb the full inflow, stationarity of the PG flow forces the surplus through the directions of smallest available area: the narrow polar funnels near $\theta \simeq 0$. This purely geometric constraint leads to a relativistic Bernoulli conversion of gravitational potential energy into axial kinetic energy,

$$\frac{E_{\rm jet}}{m} \;\sim\; \frac{A_{\rm inflow}}{A_{\rm jet}}\,\Delta\Phi,$$

and yields the long–observed fact that jets possess far larger specific energies than the surrounding winds or disks. Because stationary PG streamlines must satisfy $\dot{\theta} = 0$, they lie on cones of fixed polar angle, and the flow along these cones becomes a helical trajectory with tangent direction $\hat{e}_s \propto \hat{e}_r + \cot\theta_0\,\hat{e}_\varphi$. Thus conical collimation and helical jet morphology arise as direct consequences of the three time symmetries of the PG metric, independent of the microphysics.

This global PG backbone does not compete with magnetodynamic SMBH engines such as Blandford–Znajek or MAD/BZ jets. Instead, it complements them. In systems harbouring a spinning SMBH, the inner accretion disk and corona do not absorb all incoming PG riverlines; rather, they form a dynamical bottleneck and deflection surface that redirects a portion of the inflow into the polar funnel. The SMBH supplies electromagnetic power on horizon scales, while the PG Bernoulli geometry provides large–scale collimation, kinematic amplification, and helical streamline organisation across tens to hundreds of gravitational radii. The resulting jets are hybrids: magnetodynamic at their base but geometrically PG–Bernoulli at large scales.

This unifying picture naturally explains several universal jet properties: narrow and stable opening angles, long coherent helices, high specific energies, extreme reach relative to the galactic disk, and favourable conditions for ultra–high–energy cosmic ray acceleration. These observational features arise not from the details of the central engine, but from the global PG flow geometry shared by all matter–dominated galactic nuclei. The PG–Bernoulli framework therefore provides a common kinematic foundation on which multiple jet-launching mechanisms can build, bridging the gap between SMBH-driven models and jets appearing in younger or bulge-dominated systems.

In this sense, the PG metric offers a universal *spacetime architecture* for jet astrophysics: magnetodynamics may ignite and power the jet, but the PG–Bernoulli flow determines its large–scale shape, its collimation, its helical structure, and its ability to reach far beyond the galactic disk. Rather than competing with existing engines, the PG geometry reveals the common kinematic framework that underlies them.

References

[1] E. P. J. de Haas (2020), *Closing the Biquaternion Algebra with Gravity: Updated Construction of the Dirac Framework and the Gravitational Rotor Qg*, viXra, https://doi.org/10.5281/zenodo.17608470.

[2] E. P. J. de Haas (2025), *Metric Generation by Gravitational Rotors: Systematic Derivations and MOND Implications in a Biquaternionic Framework*, Zenodo, hhttps://doi.org/10.5281/zenodo.17573223.

[3] E. P. J. de Haas (2025), *The Qg Rotor Lagrangian: Algebraic Generation of Einstein–Cartan Dynamics*, Zenodo, https://doi.org/10.5281/zenodo.17562993.